Environ. Sci. Technol. **2002**, *36,* 1162−1168

Atmospheric Gas-Particle Partitioning of Polycyclic Aromatic Hydrocarbons in High Mountain Regions of Europe

PILAR FERNÁNDEZ,* JOAN O. GRIMALT, AND ROSA M. VILANOVA

Department of Environmental Chemistry, Institute of Chemical and Environmental Research (C.S.I.C.), Jordi Girona 18-26, 08034 Barcelona, Catalonia, Spain

Atmospheric concentrations and gas-particle partitioning of polycyclic aromatic hydrocarbons (PAH) have been determined at three remote mountain areas in Europe. Gas-phase mean concentrations of total PAH (20 individual compounds) were very similar at all sites, ranging from 1.3−2.6 ng m^{-3} in the Pyrenees (Spain) to 2.7−3.7 ng m^{-3} in the Alps (Austria) and Caledonian mountains (Norway). A seasonal variability was observed, with the highest levels found in winter. The seasonal differences were reflected better in the particle-associated PAH, showing the increase of PAH emissions in the colder months and a temperature dependence of the gas-particle partitioning. Significant geographical differences were also observed for particulate PAH, indicating a greater influence of regional sources than in the gas phase. Partitioning of PAH between gas and particulate phases was well-correlated with the subcooled liquid vapor pressure in all samples, but with slopes significantly steeper than the expected value of −1. These steeper slopes may reflect the occurrence of a nonexchangeable PAH fraction in the aerosols, likely associated to the soot carbon phase. Comparison of absorption to organic matter and soot carbon using the octanol−air (K_{oa}) and soot−air (K_{sa}) partitioning coefficients shows that, despite uncertainties on estimated organic matter and soot carbon contents in the sampled aerosols, K_{oa} underpredicts aerosol PAH concentrations by a factor of 0.6−2 log units. In contrast, predicted and measured high mountain aerosol PAH differ by 0.2−0.6 log units when K_{sa} is considered. The results point to soot carbon as the main transport medium for the long-range distribution of aerosol-associated PAH.

Introduction

Several studies have shown that a large number of semivolatile organic compounds (SOCs), including the toxic polycyclic aromatic hydrocarbons (PAH), are distributed worldwide posing at risk to both human health and ecosystem stability (*1*−*4*). Because of their volatility properties, SOCs in the atmosphere are present both in vapor form and in association to particles, mainly the fine fraction (<1 μm) (*5*, *6*), which facilitates their long-range transport (*7*−*9*).

* Corresponding author e-mail: pfrqam@iiqab.csic.es; phone: +34 93 400 6100; fax: +34 93 204 5904.

The study of SOCs in remote sites is therefore needed for the understanding of the atmospheric mechanisms involved in the long-range transport of these pollutants. Remote mountain areas, far from any pollution source and human disturbance, are unique environments for the assessment of the atmospheric pollution load over continental areas. In this respect, significant levels of SOCs have been detected in sediments and snow from remote lakes situated in high mountain areas of Europe (*2*, *10*, *11*). Their occurrence is attributed to atmospheric transport and subsequent dry and wet deposition and gas−water exchange (*12*, *13*). Gas-particle partitioning is therefore an important process for the understanding of the mechanisms leading to SOC incorporation into these lakes. Hence, there is a need to study the environmental factors controlling the levels and distributions of SOC in the air close to the lake waters.

To get an insight into this question, atmospheric samples, both gas and particulate phases, have been collected near the shore of three European remote mountain lakes during the cold and warm periods, encompassing the Catalan−Spanish Pyrenees, the Austrian Alps, and the Caledonian Mountains in Norway. Sample analysis allowed the assessment of the seasonal and spatial variability of atmospheric PAH concentrations and their phase distribution. The observed PAH partitioning was also compared with the predictions of previously reported adsorption (*14*−*16*) and absorption (*17*) models. The strong affinity between PAH and soot carbon and its influence in the atmospheric PAH distribution have been assessed by introduction of a new term for evaluation of air−soot partitioning in the absorption model (*18*). This approach provided evidence that soot carbon is very relevant for the gas-particle partitioning of these compounds and their long-range transport to remote sites.

Materials and Methods

Sampling Sites. Atmospheric samples were collected near the shore of Øvre Neådalsvatn (62°47′ N, 09°00′ E, 728 m asl, South of Norway), Gossenkölle (47°13′ N, 11°01′ E, 2413 m asl, Tyrolean Alps), and Estany Redó (42°38′ N, 0°46′ E, 2240 m asl, Catalan Pyrenees). All three lakes are situated above the local tree line. Their hydrology is only related to atmospheric precipitation (*2*). An automatic weather station (AWS) was installed at each site (30 m from lake shore and sensors 6−10 m above ground). Air temperature and pressure, wind direction and speed, solar radiation, and relative humidity were provided by the AWS every 30 min. The meteorological data collected during each sampling was averaged.

Air Sampling. Sampling was performed over 1-week periods in cold and warm weather conditions as described in Table 1. Atmospheric samples (gas and particulate matter) were collected using a high-volume air sampler (MCV, Collbató, Catalonia, Spain) equipped with glass fiber filters (GF/A, 20.3 × 25.4 cm, 1.6 μm pore size, Whatman International Ltd., Maidstone, England) and two polyurethane foam (PUF, density 28.5 kg m^{-3}, 50 mm × 65 mm i.d.) plugs inserted in a Teflon column. Samples between 80 and 170 m^3 were collected at a flow rate of 20 m^3 h^{-1}. A sample of 1000 m^3 without foam plugs was also taken in each expedition for measuring total suspended particles (TSP).

Prior to sampling, PUF plugs were cleaned by elution with Milli-Q water and acetone and were Soxhlet extracted with acetone (24 h) and *n*-hexane (48 h) until blank requirements were achieved. After preconditioning, they were dried in a vacuum desiccator, stored at room temperature in precleaned glass jars covered with aluminum foil, and

10.1021/es010190t CCC: $22.00
Published on Web 02/02/2002

TABLE 1. Sample Characteristics and Meteorological Conditions

	Redó		Gossenkölle				Øvre Neadalsvatn	
sampling period	Jul 1996	Feb 1997	Jun 1997	Oct 1996	Mar 1997	Jul 1997	Mar 1998	Jul 1998
no. of samples	2	3	7	2	4	6	5	7
TSP range (μg m^{-3})	9.4−22	15−17	6.2−46	3.9−4.9	21−31	29−56		
TSP mean (μg m^{-3})	16	16	25 (16)[a]	4.4	26	40 (22)[a]	0[a]	9.3[a]
air vol (m^3)	150−170	76−86	94−146	120−150	120−140	120−130	110−148	119−150
T range (°C)[b]	17/18	−0.9/6.4	8.0/15	2.5/4.0	−1.6/5.2	7.6/13	−13/2.0	11/20
predominant wind direction	na[c]	south/north	south	south	south	south	na	east

[a] Values in parentheses measured in 1000 m^3 sample. [b] Maximum and minimum values measured during air sampling. [c] na, not available.

sealed with Teflon film. Filters were wrapped in dichloromethane prerinsed aluminum foil and kiln-fired at 400 °C overnight. Both filter and PUF samples were frozen in the field before transport to the laboratory, where the PAH extraction were done within the following week.

Analytical Techniques. TSP for each sample was determined by filter weight difference before and after sampling. Further assessment of TSP values was obtained from 1000 m^3 volume samples collected in each sampling expedition Filters were allowed to equilibrate with ambient humidity for 24 h before weighing.

Glass fiber filters were cut into small pieces and extracted with (2:1) dichloromethane:methanol in an ultrasonic bath (3 × 25 mL, 20 min each). A mixture of anthracene-d_{10}, pyrene-d_{10}, and benzo[*ghi*]perylene-d_{12} was then added as a surrogate standard. Extracts were concentrated using a vacuum rotary evaporator to 10 mL and dried over anhydrous Na_2SO_4.

Before extraction, PUFs were spiked by injection of a mixture of naphthalene-d_8, pyrene-d_{10}, and benzo[*ghi*]-perylene-d_{12} as a surrogate standard. Twelve hours after being spiked, they were Soxhlet extracted with 400 mL of *n*-hexane for 24 h. Filters and PUFs extracts were vacuum concentrated to 1 mL and transferred to preweighed amber glass vials. Further concentration to ca. 50 μL was done under a gentle stream of nitrogen after adding 100 μL of isooctane as a keeper solvent. Vials were stored at −20 °C until instrumental analysis. Prior to injection, 50 μL of perylene-d_{12} was added as internal standard, and the vials were reweighed to obtain the total volume of dilution.

Chromatographic Analysis. PAH were quantified by gas chromatography coupled to mass spectrometry operating in electron impact and selective ion monitoring modes. A 30 m × 0.25 mm i.d. HP-5MS capillary column (film thickness of 0.25 μm) was used. Additional details of the chromatographic and spectrometric conditions are provided elsewhere (*2*). Quantification was performed by the external standard method using a PAH standard mixture (16 compounds from naphthalene to benzo[*ghi*]perylene, EPA mix, Dr. Ehrenstorfer, Augsburg, Germany). PAH concentrations were corrected by surrogate recoveries. PAH eluting between naphthalene and anthracene were corrected with anthracene-d_{10}, compounds eluting between fluoranthene and chrysene were corrected with pyrene-d_{10}, and those eluting after chrysene were corrected with benzo[*ghi*]perylene-d_{12}.

Quality Control and Assurance. Stringent precautions were taken during sampling to avoid possible contamination from the exhaust of the portable generator. Analysis of air samples taken close to it showed substantial differences in both PAH concentrations and distributions from those in long-range transported air reported in this study.

Transport, laboratory, and field blanks were processed together with the samples collected in each expedition, which involved 12 blanks (25% of the analyzed samples). Field blanks were obtained from PUF plugs and filters that were left in the high-volume pump during a complete sampling period, 4−6 h, without forcing air through them. Detection limits (DL), defined as the mean plus three times the standard deviation of the blanks values varied between 0.02 (perylene) and 4.3 ng (phenanthrene) in the particulate phase and from not detected (coronene) to 70 ng (naphthalene) in the PUF plugs (Table 2). Comparison of DL with sample levels indicates that most of the compounds are above the detection limit in more than 70% of the samples. The more volatile PAH, namely, naphthalene, acenaphthylene, and acenaphthene, show the lowest values with only 13−30% of the air samples above DL. This effect is attributed to their high volatility and consequently high dispersion in the field blank values, which increases the standard deviations and the DL for these compounds.

Breakthrough of gas-phase PAH in the air sampler was tested by separate analysis of first and second PUF in the Teflon column after collection of real samples (from Redó and Gossenkölle), with mean air volumes of 110 m^3 (5.5 h sampling time) and air temperatures in the range of −0.6 to 5 °C. For compounds with molecular weight higher than fluorene, concentrations in the second foam represented no more than 5% of the total detected level (Table 2). For more volatile PAH, this percentage increased to 30% or even more (50% in the case of naphthalene). Taking into account DL and breakthrough values, naphthalene, acenaphthylene, and acenaphthene were not included in the compilation of total PAH concentrations nor in the gas-particulate phase partitioning studies, and their reported values must be considered as semiquantitative.

Recoveries and reproducibility of the analytical procedure were evaluated from surrogate PAH results. Average recoveries were as follows: anthracene-d_{10}, 53 ± 28%; pyrene-d_{10}, 94 ± 31; and benzo[*ghi*]perylene-d_{12}, 126 ± 41% (n = 45) in the particulate phase, and 82 ± 25%, 82 ± 30%, and 91 ± 32% (n = 25), respectively, for the vapor samples. These recoveries were taken into account when reporting sample levels.

Losses of gaseous compounds in the transport from the field to the laboratory were tested by spiking PUFs with anthracene-d_{10} and transporting them together with the samples. Recoveries of this compound were high, 94 ± 18% (n = 12).

Analysis of the 80−100 m^3 and 1000 m^3 samples collected in the same sampling expeditions did not show particulate PAH concentration differences that permit the estimate of possible significant artifacts due to filter volatilization or condensation (*16*, *19*). Previous examination of possible adsorption effects into the filter by analysis of a second filter installed between the first one and the PUF showed that these could be in the level of 10% at the most, which is consistent with other reports in the literature (*16*, *19*−*21*). The present results have therefore not been corrected by adsorptions in the second filter.

Results and Discussion

Ambient Air Concentrations. The differences in PAH concentrations (gas + particulate phase) between the different sites are small and of the same order of significance as the seasonal variability (Figure 1). Mean PAH concentrations (gas

TABLE 2. Detection Limits (DL) for Individual PAH in Remote Air Samples (Aerosol and Gas Phase) and Breakthrough Evaluated by the Percentage of Each Compound in the Second PUF Plug Related to the Total PAH Content

compound	DL (ng)		% samples > DL		breakthrough % second PUF[b]
	aerosol[a]	gas phase[a]	aerosol	gas	
naphthalene (Naph)	2.99	69	13	23	53
acenaphthylene (Acyl)	3.40	4.5	30	29	39
acenaphthene (Ac)	0.36	5.7	53	81	30
fluorene (Flu)	0.70	12.5	43	100	4.8
phenanthrene (Phe)	4.27	32	47	100	3.5
anthracene (A)	0.55	3.0	30	61	4.7
fluoranthene (Fla)	0.89	3.9	80	97	1.4
acephenanthrylene (Ace)	0.11	0.37	63	74	nd[c]
pyrene (Pyr)	0.85	6.3	90	90	2.0
benzo[*a*]fluorene (B[a]flu)	0.75	nd	13	100	nd
retene (Ret)	0.29	0.28	43	87	nd
benzo[*ghi*]fluoranthene (B[ghi]fla)	1.67	0.95	40	71	nd
cyclopenta[*cd*]pyrene (Cp[cd]P)	0.19	nd	77	100	nd
benz[*a*]anthracene (B[a]A)	0.21	1.43	97	10	nd
chrysene+triphenylene (Chrys+Try)	0.41	3.43	100	10	nd
benzofluoranthenes[d] (BFlas)	0.82	2.80	100	36	nd
benzo[*e*]pyrene (B[e]P)	0.27	1.54	100	48	nd
benzo[*a*]pyrene (B[a]P)	0.19	0.99	100	35	nd
perylene (Per)	0.02	0.04	100	45	nd
indeno[7,1,2,3-*cdef*]chrysene (IChrys)	0.19	0.14	90	48	nd
indeno[1,2,3-*cd*]pyrene (IPyr)	0.34	0.77	93	42	nd
dibenz[*ah*]anthracene (DB[ah]A	0.07	0.77	87	42	nd
benzo[*ghi*]perylene (B[ghi]Per)	0.57	1.02	87	42	nd
coronene (Cor)	0.18	nd	93	100	nd
total PAH[e]	21	58	50	100	4.1

[a] Calculated as the mean ± SD of field blanks levels ($n = 12$) in all sites. [b] Average of two samples, mean volume 110 m^3 (5.5 h). [c] nd, below instrumental detection limit. [d] Sum of *b, j, k*, and *a* isomers. [e] Sum of all compounds except Naph, Acyl, Ac, and Ret.

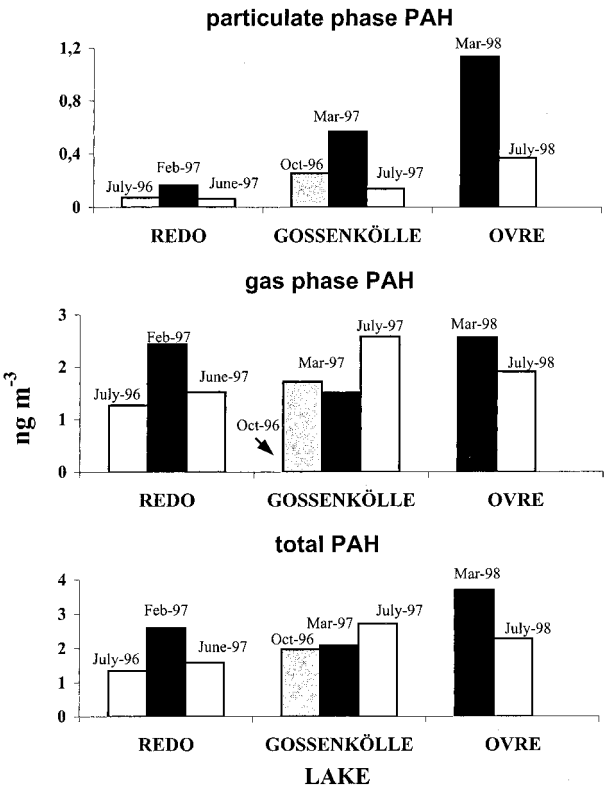

FIGURE 1. Total concentrations of atmospheric PAH (sum of the 20 compounds listed in Table 2).

+ particles) ranged between 1.3−2.6 ng m^{-3} in Redó and 2.0−3.7 ng m^{-3} in Gossenkölle and Øvre Neådalsvatn. Total PAH levels in the atmosphere of these remote lakes were between those typically detected in urban air (about 2 or 3 orders of magnitude higher) and those reported in the Arctic (0.19−0.47 ng m^{-3}) (*22*). They are consistent with PAH concentrations found in other remote continental areas such as Lake Superior (2.9−3.9 ng m^{-3}) (*7, 13*) or rural sites, e.g., Chesapeake Bay (2.7−5.3 ng m^{-3}) (*12, 20*).

Gas-phase PAH concentrations are 1 order of magnitude higher than the particle-associated compounds in Gossenkölle and Redó and between a factor of 2 and 5 in Øvre Neådalsvatn. The qualitative distributions in this phase are similar at the three sites (Figure 2), being dominated by phenanthrene (45−70% of total PAH), fluorene (20−30%), fluoranthene (7−16%), and pyrene (2−10%). Gas-phase PAH with higher molecular weight than pyrene only accounted for 1−6%.

The PAH concentrations in the particulate phase range between 65 and 1100 pg m^{-3}. The highest levels occur in winter, consistently with the increase in PAH emissions to the atmosphere in cool periods and to the longer pathway of air masses over continental Europe or the British Islands than in summer, as revealed from compilation of the backward air mass trajectories. Aerosol PAH concentrations of 12 pg m^{-3} have been reported in the North Pacific (*23*), 8−400 pg m^{-3} in the central western Mediterranean Basin (*24, 25*), and 300−27000 pg m^{-3} in Corsica (*26*). Higher levels of particulate-phase PAH are found in Øvre Neådalsvatn than in Redó and Gossenkölle (Figure 1). The Norwegian site is the one showing a more different distribution with a higher contribution of the PAH with 5−6 rings than in the other lakes. Hence, chrysene, benzofluoranthenes, benzo[*e*]pyrene, and phenanthrene accounted for 33−58% of total PAH. In Redó and Gossenkölle, aerosol PAH are dominated by phenanthrene, being closer to the gas-phase distribution but with a higher proportion of the higher molecular weight components (Figure 2).

The distinct features of air PAH distributions in Øvre Neådalsvatn are consistent with the differences in aquatic PAH between these three lakes (*27*). Higher relative proportions of 5−6 ring PAH were found in Øvre Neådalsvatn waters than in Redó and Gossenkölle. The high proportion of these

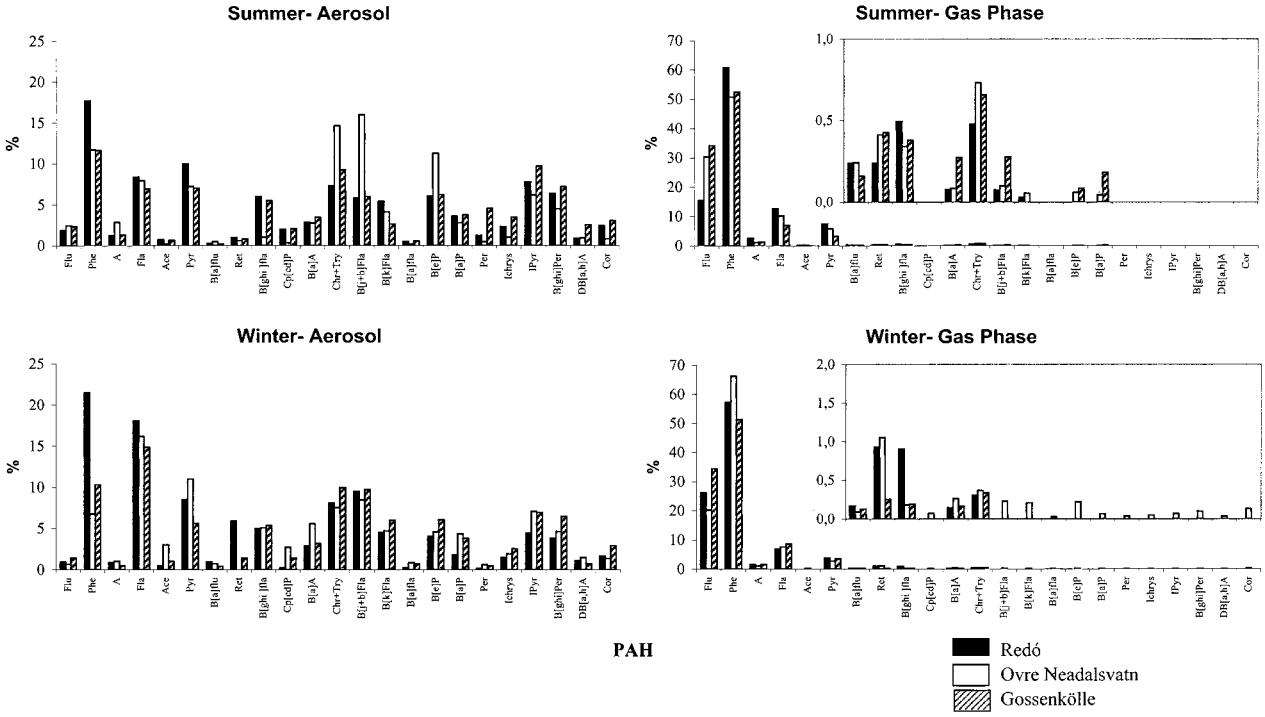

FIGURE 2. PAH composition in the aerosol and gas phase of the air samples collected in the high mountain areas considered for study. The results are expressed as percentage of each individual compound related to total PAH as defined in Table 2. Compound identification in Table 2.

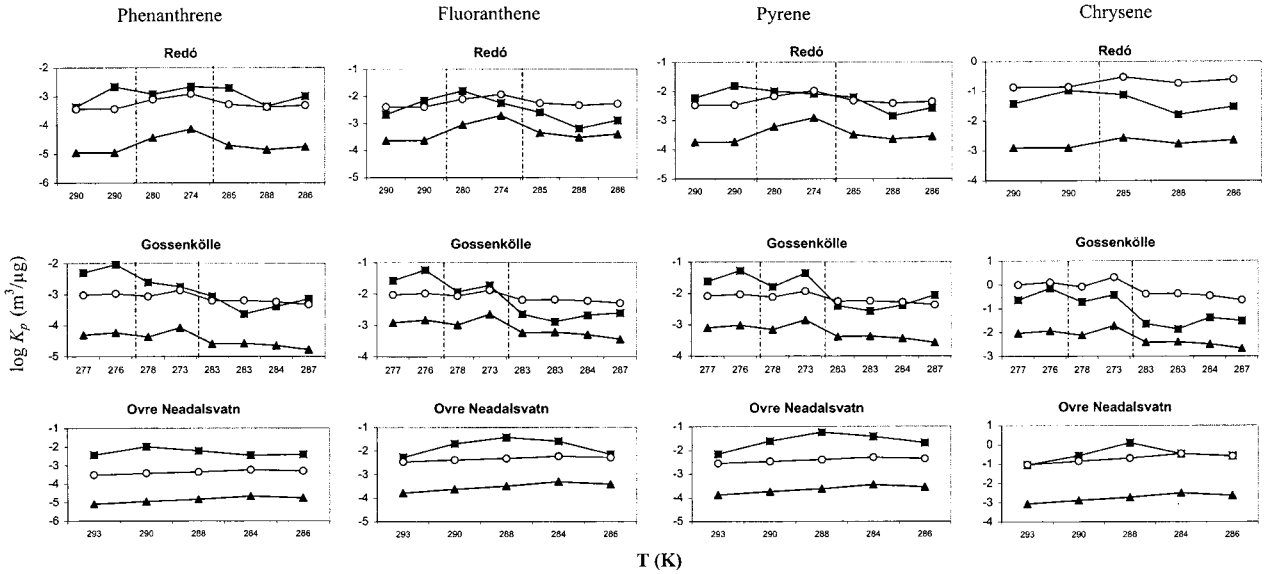

FIGURE 3. Experimental and predicted K_p values ($m^3\ \mu g^{-1}$) in the air from remote mountain areas: (■) measured; (▲) predicted from K_{oa} values (eq 3) assuming 10% of aerosol organic matter; (○) predicted by K_{oa} and K_{sa} model (eq 5) assuming 10% and 3% of organic matter and elemental carbon in atmospheric aerosols, respectively. Vertical dotted lines separate different sampling periods: Redó, July 1996, February 1997 (Chrys below detection limit in the gas phase), and June 1997; Gossenkölle, October 1996, March 1997, and July 1997.

PAH in Øvre Neådalsvatn is consistent with previous reports on PAH composition in long-range transported aerosols collected in Norway and has been attributed to inputs from the British Islands as well as from the European continent (*28*, *29*).

Gas-Particle Partitioning of PAH. Phenanthrene, anthracene, fluoranthene, pyrene, benz[*a*]anthracene, and chrysene have been taken as model compounds for the study of the gas-phase partitioning of PAH in these high mountain atmospheres since they have concentrations well above the detection limit in both gas and particulate phases, and they are not affected by sampling or analytical problems. The concentrations of these compounds in these two phases have been used for calculating the partition coefficient K_{pi} ($m^3\ \mu g^{-1}$), defined as $K_{pi} = C_{pi}/(C_{gi} \times \mathrm{TSP})$, where C_{pi} and C_{gi} (pg m^{-3}) are the equilibrium concentrations of compound i in the particle and gas phase, respectively (Figure 3).

A linear fit between K_{pi} and the subcooled liquid vapor pressure p°_{Li} (Torr) of a specific compound class has often been observed (*14*) according to the general expression

$$\log K_{pi} = m \log p^{\circ}_{Li} + b \qquad (1)$$

As summarized in Table 3, significant linear correlation

TABLE 3. Observed Regression Coefficients for Log K_p ($m^3\ \mu g^{-1}$) vs Log p_L° [a] (Torr) (Eq 1) for Selected PAH[b] in Air Samples from Remote Mountain Areas

site	*n*	slope	*b*	R^2
Redó				
all samples	9	−0.630 ± 0.045	−5.458 ± 0.224	0.771
July 1996	2	−0.610 ± 0.082	−4.942 ± 0.387	0.823
February 1997	2	−0.603 ± 0.067	−5.451 ± 0.350	0.890
June 1997	5	−0.685 ± 0.054	−5.854 ± 0.274	0.829
Gossenkölle				
all samples	9	−0.560 ± 0.041	−5.245 ± 0.251	0.705
October 1996	2	−0.508 ± 0.038	−4.284 ± 0.252	0.893
March 1997	3	−0.650 ± 0.057	−5.413 ± 0.325	0.901
July 1997	4	−0.516 ± 0.031	−5.469 ± 0.189	0.875
Øvre Neådalsvatn				
July 1998	6	−0.564 ± 0.045	−4.344 ± 0.258	0.717
urban (Chicago) (*17*)	15	−0.745		0.999
urban (Denver) (*46*)		−0.76		
over Lake Michigan (*21*)	17	−0.665		0.830
Chesapeake Bay (urban) (*20*)	5	−1.03 ± 0.19	−10.9 ± 1.2	0.87
Chesapeake Bay (rural) (*20*)	10	−0.649 ± 0.209	−7.67 ± 1.19	0.83
Lake Superior (rural) (*7*)		−0.59		
Manchester (urban) (*47*)	9	−0.72	−5.2	0.96
rural (U.K.) (*47*)	9	−0.79	−5.3	0.97

[a] p_L° corrected by mean temperature of each sample as described in ref *48* and revised by Pankow and Bidleman (*15*). [b] Phenanthrene, anthracene, fluoranthene, pyrene, benz[*a*]anthracene, and chrysene.

coefficients ($r^2 = 0.717-0.705$; $p < 0.0001$) have been obtained for all sites. These coefficients are even higher when the results examined correspond to those obtained in single sampling series, e.g., $r^2 = 0.905-0.959$ in Gossenkölle, 0.831−0.955 in Redó, and 0.749−0.938 in Øvre Neådalsvatn. These good linear correlations agree with the linear isotherm model for the partitioning of airborne pollutants between gas and particulate phases (*14*, *15*, *30*) suggesting that, as expected, C_{gi} and C_{pi} were in equilibrium in these long-range transported air samples.

However, this equilibrium condition also requires a slope of $m = -1$ (*14*, *15*, *30*), which is not observed. *m* values and intercepts varied between samples but in all cases the slopes were higher than −1, in the range of −0.508 to −0.685 (Table 3), indicating a higher PAH content in the particulate phase than that predicted by the Junge−Pankow model. In fact, slopes deviating from −1 are very frequent in the literature (see Table 3), commonly attributed to nonequilibrium conditions or sampling artifacts. *m* values higher than −1 are more often encountered in rural and remote atmospheres than in urban air (*20*, *21*), which is a priori surprising since gas and particle PAH concentrations in remote atmospheres must be closer to equilibrium conditions than in urban air because they have been transported over long distances from their sources (*16*, *31*). Recently, it has been reported than *m* values deviating from −1 are not always indicative of nonequilibrium conditions (*21*, *32*).

Variations in atmospheric temperature and concentration during sampling are unlikely to explain these deviations since each sampling lasted for 4−5 h, and significant concentration changes are not expected during these short periods. In situ temperature was measured every 30 min and varied by no more than 3−4 °C during each collection period.

The occurrence of a nonexchangeable PAH fraction in the aerosols can account for the shallower slopes observed in our study. Since these compounds originate primarily in combustion processes, they can be trapped irreversibly in the soot matrix. This would lead to a PAH fraction in the aerosols only partially available for partitioning to the gas phase (*20*, *33*), enhancing their concentration in the particulate matter.

In fact, *m* values can also provide insight into the mechanism driving gas-particle partitioning (*32*). Slopes steeper than −1 are characteristic of adsorption on particle surfaces, while those shallower than −0.6 point to absorption into aerosol organic matter. In Gossenkölle and Øvre Neådalsvatn, *m* values are slightly lower than −0.6, which could be consistent with the absorption mechanism. Slopes in the range of −0.6 and −1, as those observed in Redó, are intermediate and do not allow such a distinction.

Absorption on Organic Matter. Octanol−air partitioning coefficients, K_{oa}, are better descriptors of the gas-particle partitioning than p_L° when absorption is the predominant gas-particle distribution process (*34*). Recently, K_{oa} values have been used for description of the gas-particle distribution of PAH in urban air of Chicago (*17*). The logarithmic form of the relationship between K_p and K_{oa} can be written as (*34*)

$$\log K_p\ (m^3\ \mu g^{-1}) = \log K_{oa} + \log f_{om} + \log(10^{-12}(\gamma_{oct}/\gamma_{om})(M_{oct}/M_{om})/\rho_{oct}) \quad (2)$$

where f_{om} is the fraction of organic matter in the collected particles; γ_{oct} and γ_{om} are the activity coefficients of the absorbing compound in octanol and particulate organic matter, respectively; M_{oct} and M_{om} are the molecular weights of octanol and the organic matter; and ρ_{oct} is the density of octanol (0.820 kg L^{-1}).

Good linear correlations have been found in the curve fitting of observed log K_p vs temperature-corrected log K_{oa} (*35*) (Table 4) with r^2 values between 0.556 (Redó, $p < 0.001$) and 0.752 (Gossenkölle, $p < 0.001$). However, the slopes encountered are significantly smaller than 1, at least in Redó and Øvre Neådalsvatn which, assuming similar sorbing properties between octanol and sampled air particles, indicates the occurrence of another mechanism besides pure absorption.

Assuming that γ_{oct}/γ_{om} and $M_{oct}/M_{om} = 1$, eq 2 can be written as

$$\log K_p\ (m^3\ \mu g^{-1}) = \log K_{oa} + \log f_{om} - 11.91 \quad (3)$$

This equation can be used to predict values of K_p if the organic matter fraction f_{om} of the aerosols are known and assuming that all of the particle organic matter is available to absorb gas-phase compounds. It has been reported that organic carbon varies between 0.21 and 0.80 μg of C m^{-3} in aerosols of remote marine areas of the Northern Hemisphere (*36*)

TABLE 4. Observed Regression Coefficients for Log K_p (m^3 μg^{-1}) vs Log K_{oa}[a] (Eq 3) for Selected PAH[b] in Air Samples from Remote Mountain Areas

site	*n*	slope	*b*	R^2
Redó				
all samples	8	0.621 ± 0.098	−8.153 ± 0.924	0.556
July 1996	2	0.838 ± 0.195	−9.793 ± 1.780	0.755
February 1997	2	0.593 ± 0.109	−7.900 ± 1.064	0.856
June 1997	4	0.684 ± 0.170	−8.851 ± 1.594	0.617
Gossenkölle				
all samples	9	0.930 ± 0.116	−11.143 ± 1.128	0.681
October 1996	2	0.767 ± 0.103	−8.924 ± 1.020	0.902
March 1997	3	0.876 ± 0.106	−10.355 ± 1.051	0.920
July 1997	4	0.737 ± 0.101	−9.74 ± 0.959	0.791
Øvre Neådalsvatn				
July 1998	6	0.771 ± 0.135	−8.810 ± 1.247	0.598

[a] K_{oa} corrected by mean temperature of each sample as described in ref *35* for Phe, Fla, and Pyr. For Chrys, $K_{oa} = K_{ow}RT/H$, where K_{ow} is the octanol−water partitioning coefficient from ref *49*, R is the ideal gas constant (8.3144 Pa m^3 mol^{-1} K^{-1}), T is absolute temperature (K), and H is the Henry law constant corrected by mean temperature as described in ref *44*. [b] Phenanthrene, fluoranthene, pyrene, and chrysene.

with TSP values around 10 μg m^{-3} (2−8% of the organic carbon). Transformation of these values into organic matter leads to 3−11% (assuming the same carbon percentage for organic compounds and octanol; *17*). The upper values of this range are expected for continental remote areas. Therefore, f_{om} has been estimated at 10% for K_p prediction with eq 3. As shown in Figure 3, despite the good correlation between log K_p and log K_{oa}, there is a shift between measured and predicted K_p values, the later being 1−2 orders of magnitude lower. The differences cannot be attributed to the selected f_{om} since a sensible modification would require the introduction of unrealistic values, 1 order of magnitude higher. Again, the differences point to a higher PAH concentration in the particulate matter than that predicted by the absorption model, consistent with the occurrence of a nonexchangeable PAH fraction in the aerosols.

Sorption on Organic Carbon. The strong association of PAH with soot particles in the aquatic environment has recently been described (*37*−*39*). A soot carbon-normalized partition coefficient, K_{sw}, extending the hydrophobic partition model to the inclusion of sorption with soot carbon phase has been developed (*38*):

$$K_d = f_{oc}K_{oc} + f_{sc}K_{sw} \quad (4)$$

where f_{oc} and f_{sc} are the fractions of organic matter and soot carbon in the water particulate matter, respectively, and K_{oc} is the organic carbon-normalized equilibrium coefficient.

At the low concentrations found in aquatic systems, the K_{sw} values can be estimated from the activated carbon−water partition coefficient (*40*, *41*). Since both PAH and soot material are generated in combustion sources, they are present concurrently in the atmosphere. The high affinity of PAH for soot material has been reported from laboratory sorption studies based on carbon black and activated carbon (*37*, *41*). Association between PAH and the soot phase likely takes place in the atmosphere before deposition to the aquatic systems. In fact, it is commonly accepted that pyrolytic PAH adsorb on soot surfaces, preventing degradation in the atmosphere, as well as in the water column and sediments (*42*, *43*).

The soot partition model for aquatic systems has recently been extended to gas-particle partitioning of PAH in the atmosphere (*18*). The soot−air partition coefficient K_{sa} (L kg^{-1}) can be defined as $K_{sa} = K_{sw}/H'$ where H' is the dimensionless Henry's law constant at a given temperature (*44*) and K_{sw} is the activated carbon−water partition coefficient (*41*).

The gas-particle equation describing organic matter absorption and soot carbon adsorption is given by

$$K_p = \frac{f_{om}MW_{oct}\gamma_{oct}}{\rho_{oct}MW_{om}\gamma_{om} \times 10^{12}}K_{oa} + f_{EC}\frac{a_{ec}}{a_{ac} \times 10^{12}}K_{sa} \quad (5)$$

where f_{EC} is the fraction of elemental carbon in the atmospheric particles, used as a surrogate for the soot carbon phase; a_{ac} is the surface area of activated carbon; a_{ec} is the specific surface area of elemental carbon; and 10^{12} is a factor for units correction. Assuming that the ratios γ_{oct}/γ_{om}, M_{oct}/M_{om}, and a_{ec}/a_{ac} are equal to 1, it is possible to predict K_p values if f_{om} and f_{EC} are known.

A total carbon to elemental carbon ratio of 1.8 has been described for urban aerosols (*17*), which increases to 2−4 for air masses aged due to aerosol mixing with noncombustion particles and condensation of material from the gas phase (*36*). This ratio corresponds to elemental carbon values in the range of 2−4% (assuming an organic carbon content of 8% in the aerosols studied). For TSP values in these remote areas ranging between 4 and 40 μg m^{-3}, an average value of 3% of elemental carbon would give a soot concentration between 0.12 and 1.2 μg m^{-3}, consistent with the values reported for rural and remote areas between 0.2 and 2.0 μg m^{-3} (*36*). f_{EC} values of 0.03 are therefore a good estimate of the elemental carbon content in the aerosols of these remote mountain areas.

Calculations of K_p as defined in eq 5 using these assumptions result in a close resemblance with the measured values in all samples and sites (Figure 3). The paired *t*-test between measured and calculated K_p indicates no significant difference within a 95% confidence interval in the three areas. Nevertheless, some discrepancies can be observed for fluoranthene and chrysene in Lakes Redó and Gossenkölle in the summer of 1997. These differences are likely a consequence of the variations in the chemical composition of atmospheric particles, not reflected by the uniform f_{om} and f_{EC} values used, which could have more influence in the compounds with highest partition coefficients. Another possible source of discrepancy can be temperature. Temperature variations have been taken into account in part when using temperature-corrected values of H' for K_{sa}. However, K_{sw} must be temperature-dependent, and this dependency has not been evaluated because 298 K reference values (*41*) were used.

Uncertainties in K_{sw} values also influence the results. In this sense, K_{sw} values 1 log unit lower than those used in this study have been reported recently (*45*). Despite these limitations, the good agreement between predicted and measured K_p values evidence that soot carbon plays an important role in PAH partitioning and long-range transport of these compounds to high mountain areas. The soot−air partitioning coefficients found for these compounds are high, K_{sa} values ranging between 10^{-2} (phenanthrene) and 10^2 m^3 μg^{-1} (chrysene) (2−3 orders of magnitude higher than K_{oa}) pointing out to a stronger association between soot and PAH than with organic matter. Accordingly, the slopes values deviating from −1 in the log K_p vs log $p°_L$ plots observed in this and other studies may be a consequence of this soot−PAH association, resulting into the so-called nonexchangeable PAH fraction in the atmospheric particles.

As observed in the present study, this effect must be more important in remote areas since only the most refractory soot-associated PAH can survive to the long-range atmospheric transport. Future studies on fate and transport of these hydrocarbons should consider that the global distribution of particulate PAH depends on transport on soot carbon phases.

Acknowledgments

We thank Guillem Carrera for his valuable help in sampling. Field support by Ulrike Nickus, Hansjörg Thies (University of Innsbruck), Marc Ventura, Lluis Camarero, Jordi Catalan (University of Barcelona), and Leif Lien (NIVA, Norway) is also acknowledged. Carolina Martínez is thanked for the analyses of samples from Øvre Neådalsvatn. Meteorological data have been provided by Ulrike Nickus (University of Innsbruck) and David Livingstone (EAWAG, Dübendorf). We also thank Roser Chaler for technical assistance in instrumental analysis. Financial support from the European Union, MOLAR (ENV4-CT95-0007) and EMERGE (EVK1-CT-1999-00032) projects, is acknowledged. R.M.V. thanks the Spanish Ministry of Education for a Ph.D. fellowship.

Literature Cited

(1) Wania, F.; Mackay, D. *Ambio* **1993**, *22*, 10−18.
(2) Fernández, P.; Vilanova, R. M.; Grimalt, J. O. *Environ. Sci. Technol.* **1999**, *33*, 3716−3722.
(3) Gregor, D. J.; Gummer, W. D. *Environ. Sci. Technol.* **1989**, *23*, 561−565.
(4) LaFlamme, R. E.; Hites, R. A. *Geochim. Cosmochim. Acta* **1978**, *42*, 289−303.
(5) Aceves, M.; Grimalt, J. O. *Environ. Sci. Technol.* **1993**, *27*, 2896−2908.
(6) Allen, J. O.; Dookeran, N. M.; Smith, K. A.; Sarofim, A. F.; Taghizadeh, K.; Lafleur, A. L. *Environ. Sci. Technol.* **1996**, *30*, 1023−1031.
(7) McVeety, B. D.; Hites, R. A. *Atmos. Environ.* **1988**, *22*, 511−536.
(8) Atlas, E.; Foster, R.; Giam, C. S. *Science* **1981**, *211*, 163−165.
(9) Grimalt, J. O.; Albaigés, J.; Sicre, M. A.; Marty, J. C.; Saliot, A. *Naturwissenschaften* **1988**, *75*, 39−42.
(10) Fernández, P.; Vilanova, R. M.; Martínez, C.; Appleby, P.; Grimalt, J. O. *Environ. Sci. Technol.* **2000**, *34*, 1906−1913.
(11) Carrera, G.; Fernández, P.; Vilanova, R. M.; Grimalt, J. O. *Atmos. Environ.* **2001**, *35*, 245−254.
(12) Leister, D. L.; Baker, J. E. *Atmos. Environ.* **1994**, *28*, 1499−1520.
(13) Baker, J. E.; Eisenreich, S. J. *Environ. Sci. Technol.* **1990**, *24*, 342−352.
(14) Pankow, J. F. *Atmos. Environ.* **1987**, *21*, 2275−2283.
(15) Pankow, J. F.; Bidleman, T. F. *Atmos. Environ.* **1992**, *26A*, 1071−1080.
(16) Cotham, W. E.; Bidleman, T. F. *Environ. Sci. Technol.* **1995**, *29*, 2782−2789.
(17) Harner, T.; Bidleman, T. F. *Environ. Sci. Technol.* **1998**, *32*, 1494−1502.
(18) Dachs, J.; Eisenreich, S. J. *Environ. Sci. Technol.* **2000**, *34*, 3690−3697.
(19) Cotham, W. E.; Bidleman, T. F. *Environ. Sci. Technol.* **1992**, *26*, 469−478.
(20) Gustafson, K. E.; Dickhut, R. M. *Environ. Sci. Technol.* **1997**, *31*, 140−147.
(21) Simcik, M. F.; Franz, T. P.; Zhang, H.; Eisenreich, S. J. *Environ. Sci. Technol.* **1998**, *32*, 251−257.
(22) Halsall, C. J.; Barrie, L. A.; Fellin, P.; Muir, D. C. G.; Billeck, B. N.; Lockhart, L.; Rovinsky, F. Y.; Kononov, E. Y.; Pastukhov, B. *Environ. Sci. Technol.* **1997**, *31*, 3593−3599.
(23) Atlas, E. In *The Long-Range Atmospheric Transport of Natural Contaminants and Substances*; Knap, A. H., Ed.; Kluwer Academic: Dordrecht, The Netherlands, 1990; pp 105−135.
(24) Sicre, M. A.; Marty, J. C.; Saliot, A.; Aparicio, X.; Grimalt, J.; Albaigés, J. *Atmos. Environ.* **1987**, *21*, 2247−2259.
(25) Simó, R.; Colom-Altes, M.; Grimalt, J. O.; Albaigés, J. *Atmos. Environ.* **1991**, *25A*, 1463−1471.
(26) Masclet, P.; Pistikopoulos, P.; Beyne, S.; Mouvier, G. *Atmos. Environ.* **1988**, *22*, 639−650.
(27) Vilanova, R. M.; Fernandez, P.; Martinez, C.; Grimalt, J. O. *Water Res.* **2001**, *35*, 3916−3926.
(28) Lunde, G.; Björseth, A. *Nature* **1977**, *268*, 518−519.
(29) Björseth, A.; Lunde, G. *Atmos. Environ.* **1979**, *13*, 45−53.
(30) Junge, C. E. In *Fate of Pollutants in the Air and Water Environments*; Suffet, I. H., Ed.; Wiley-Interscience: New York, 1977; pp 7−26.
(31) Kamens, R.; Odum, J.; Fan, Z.-H. *Environ. Sci. Technol.* **1995**, *29*, 43−50.
(32) Goss, K.-U.; Schwarzenbach, R. P. *Environ. Sci. Technol.* **1998**, *32*, 2025−2032.
(33) Simó, R.; Grimalt, J. O.; Albaigés, J. *Environ. Sci. Technol.* **1997**, *31*, 2697−2700.
(34) Finizio, A.; Mackay, D.; Bidleman, T.; Harner, T. *Atmos. Environ.* **1997**, *31*, 2289−2296.
(35) Harner, T.; Bidleman, T. F. *J. Chem. Eng. Data* **1998**, *43*, 40−46.
(36) Seinfeld, J. H.; Pandis, S. N. *Atmospheric Chemistry and Physics. From Air Pollution to Climate Change*; John Wiley & Sons: New York, 1997.
(37) Gustafsson, Ö.; Gschwend, P. M. In *Molecular Markers in Environmental Geochemistry*; Eganhouse, R. P., Ed.; ACS Symposium Series 671; American Chemical Society: Washington, DC, 1997; pp 365−381.
(38) Gustafsson, O.; Haghseta, F.; Chan, C.; MacFarlane, J.; Gschwend, P. M. *Environ. Sci. Technol.* **1997**, *31*, 203−209.
(39) Jonker, M. T. O.; Smedes, F. *Environ. Sci. Technol.* **2000**, *34*, 1620−1626.
(40) Luehrs, D. C.; Hickey, J. P.; Nilsen, P. E.; Godbole, K. A.; Rogers, T. N. *Environ. Sci. Technol.* **1996**, *30*, 143.
(41) Walters, R. W.; Luthy, R. G. *Environ. Sci. Technol.* **1984**, *18*, 395−403.
(42) Baker, J. E.; Eisenreich, S. J.; Eadie, B. J. *Environ. Sci. Technol.* **1991**, *25*, 500−509.
(43) Lipiatou, E.; Marty, J. C.; Saliot, A. *Mar. Chem.* **1993**, *44*, 43−54.
(44) Bamford, H. A.; Poster, D. L.; Baker, J. E. *Environ. Toxicol. Chem.* **1999**, *18*, 1905−1912.
(45) Bucheli, T. D.; Gustafsson, Ö. *Environ. Sci. Technol.* **2000**, *34*, 5144−5151.
(46) Foreman, W. T.; Bidleman, T. F. *Atmos. Environ.* **1990**, *24A*, 2405−2416.
(47) Lohmann, R.; Harner, T.; Thomas, G. O.; Jones, K. C. *Environ. Sci. Technol.* **2000**, *34*, 4943−4951.
(48) Yamasaki, H.; Kuwata, K.; Kuge, Y. *Nippon Kagaku Kaishi* **1984**, *8*, 1324−1329.
(49) Mackay, D.; Shiu, W. Y.; Ma, K. C. *Physical−Chemical Properties and Environmental Fate Handbook*; CRC Press: Boca Raton, FL, 1999.

Received for review July 26, 2001. Revised manuscript received November 28, 2001. Accepted November 29, 2001.

ES010190T